On-orbit spatial resolution estimation of CBERS-1 CCD imaging system using higher resolution images

Kamel Bensebaa
Gerald Jean Francis Banon
Leila Maria Garcia Fonseca

Image Processing Division - National Institute for Space Research (INPE)
Av. dos Astronautas, 1758, 12227-010 São José dos Campos, Brazil
{camel, banon, leila}@dpi.inpe.br

Abstract. The first China-Brazil Earth Resources Satellite (CBERS-1) was launched in 1999 and in 2003 was substituted by CBERS-2. CBERS-1 and CBERS-2 have the same specifications and carry three sensors: WFI, CCD and IR-MSS. The performance of these sensors can be evaluated through PSF measurement that enables an objective assessment of the spatial resolution. This paper describes an approach to estimate the spatial resolution of the CBERS-1 CCD camera using two images: an image captured by CBERS-1 satellite and an image of the same scene of higher resolution captured by SPOT-4 satellite The method is iterative and the goal is to find the low-pass band filter parameter that minimizes the Root Mean Square (RMS) difference between the CBERS-1 image and the filtered SPOT-4 one. This technique is applied to spatial resolution estimation in across-track direction using an image of Lake Pontchartrain Causeway in Louisiana (United States), and, in along-track direction using an image of Rio-Niteroi Bridge in Rio de Janeiro (Brazil).

Keywords: CBERS-1 satellite, SPOT-4 satellite**,** CCD camera, spatial resolution, point spread function, estimation, modelling, simulation, measurement.

1. Introduction

In the last two decades China and Brazil have jointly developed through a cooperative program, the CBERS satellite (China-Brazil Earth Resources Satellite). The CBERS-1 and CBERS-2 satellites were launched on October 14, 1999 and October 21, 2003, respectively by the Chinese launcher Long-March 4B, from the Tayuan Launch Center, in the Popular Republic of China. The main objective of CBERS mission is to obtain global, regional, and local images of the Earth in four different wavelengths of the electromagnetic spectrum (spectral bands), ranging from visible to infrared light.

The CBERS-1 payload consists of three instruments called: CCD (Charge Coupled Device) camera, IRMSS (Infrared MSS) and WFI (Wide Field Imager), which can capture otical observation of the Earth surface and transmit remotely sensed data to ground receiving stations.

During the acquisition process, the imaging system causes image degradations due to the cumulative effects of the instrumental optics (diffraction, aberrations, focusing error) and image motion induced by the satellite movement (Leger et al. 2002). Typically, the degradation can be modeled by linear system characterized by its Point Spread Function (PSF) or by its Modulation Transfer Function (MTF) in the frequency domain.

According to the literature, the PSF can be approximated by a Gaussian function (Luxen and Forster, 2002). Hence, in this work the PSF is modeled as two one-dimensional Gaussian functions: one relative to the along-track direction and the second one to the across-track direction.

The point spread function (PSF) of a given image acquisition system measure how the optical system spreads the image of a point, and it enables an objective assessment of the imaging system spatial resolution parameter. In remote sensing, the spatial resolution parameter is known as EIFOV and enables a comparison between different sensors. When the

PSF is approximated by a Gaussian function with standard deviation σ, the EIFOV is 2.66σ (Slater, 1980; Banon and Santos, 1993).

In this work, our goal is to estimate the spatial resolution using images from different sensors. SPOT-4 images have been chosen as a reference because they have slightly better resolution than the CBERS-1 images (Bensebaa, et al, 2004b), they have the same sampling rate. Furthemore, SPOT-4 EIFOVs are known and are used in CBERS-1 EIFOVs estimation. The method is iterative and consists of finding the low-pass band filter parameter that minimizes the Root Mean Square (RMS) difference between the CBERS-1 image and the filtered SPOT-4 one This technique is applied to spatial resolution estimation in across-track direction using image of Lake Pontchartrain Causeway in Louisiana (United States), and, in along-track direction using image of Rio-Niteroi Bridge in Rio de Janeiro (Brazil).

2. CBERS-1 overview

The CBERS-1 satellite carries on-board a multisensor payload with different spatial resolution called: WFI (Wide Field Imager), IRMSS (Infrared MSS) and CCD (Charge Coupled Device) camera. The high-resolution CCD Camera has 4 spectral bands from visible light to near infrared and one panchromatic band (**Table 1**). It acquires the earth ground scenes by pushbroom scanning, on 778 km sun-synchronous orbit and provides images of 113 km wide strips with sampling rate of 20 meters at nadir Dayao et al. (2001).

Table 1. Spectral bands of the CCD sensor.

Spectral Bands	Number	Wavelength (μm)
Blue	B1	0,45 - 0,52
Green	B2	0,52 - 0,59
Red	B3	0,63 - 0,69
Near-Infrared	B4	0,77 - 0,89
Pan.	B5	0,51 - 0,73

The signal acquisition system operates in two channels called CCD1 and CCD2. The first one generates images corresponding to B2, B3 and B4 while the second generates images corresponding to the bands B1, B3 and B5. In each channel (channel C1 and channel C2), three CCD chips per band were combined to generate about 6000 pixels per row.

3. Point spread function (PSF) estimation methodology

The PSF estimation is a general tool for assessment of the imaging system performance. Basically, there exist three ways to determinate the PSF. The first one uses images targets that must have well-defined shape and size as airport runway, bridges, etc or artificial target. The second method utilizes images acquired by higher resolution sensor, which are low-pass filtered and compared with the image under study (see Banon (1990) for a simulation study). Finally, the third one uses the system design specifications and the system analytic model (Fonseca, 1987; Fonseca and Mascarenhas, 1987).

The first two approaches have the advantage of estimating the imaging system PSF by using in-flight images. Previous works dealing with this problem have obtained satisfactory results using the first approach. Storey (2001) has used this methodology to measure the Landsat-TM on-orbit spatial response using ground target such as bridges. Choi and Helder (2001) have used as targets airport runway and a tarp placed on the ground for on-orbit MTF measurement of IKONOS satellite sensor. Bensebaa et al. (2004b) have used bridges images to estimate the spatial resolution of CBERS-1 imaging system. The spatial resolution estimation used in this work is based on the second approach.

3.1 Target selection

The image selection was made based on separability properties. In order to make profit of the simplicity of working with 1D data, we chose images of along-track and across-track bridges, which are typically 1D, target. The Rio-Niteroi Bridge over Guanabara Bay (**Figure 1** and **Figure 3**) was chosen as 1D target to estimate the spatial resolution in the along-track direction. This bridge is 13.29-km long with only one deck and its width is 26.6 meters. On the other side, the Causeway Bridge over the Lake Pontchartrain (**Figure 2** and **Figure 4**) was used as 1D target to estimate the spatial resolution in across-track direction. The target is a 38.62-km long double deck bridge where each deck is 10.0 meters width and the gap is 24.4 meters width. The two decks of the bridge were constructed at different times (1956 and 1969) and exhibit slightly different reflectance. In addition, the water background is reasonably uniform.

3.2 Data preparation

The Rio-Niteroi bridge and Lake Pontchartrain Causeway bridge images were acquired by CBERS-1 CCD sensor on December 02, 2001 and October 06, 2002, respectively. The same scenes were acquired by SPOT-4 CCD on November 28, 2001 for Rio-Niteroi Bridge and on November 25, 2002 for Lake Pontchartrain Causeway Bridge.

The CBERS-1 raw data images present a striping effect. Odd columns are brighter than even columns. This is due to the non-uniform detector gains, since each detector is responsible for one column in the images. The processing procedure to remove the stripping effect has been described in (Bensebaa, et al. 2004a). **Figure 5** and **Figure 7** shows destriped images of Band2 captured by CBERS-1 satellite CCD while **Figure 6** and **Figure 8** shows images of Band2 captured by SPOT-4 satellite CCD.

3.3 Image registration

As the scenes images of Rio-Niteroi bridge and Causeway bridge were captured by different sensors, we have applied the registration algorithm developed by (Fedorov, et al, 2002). The SPOT-4 images were used as reference. **Figures 9** and **Figures 10** show the results of this processing.

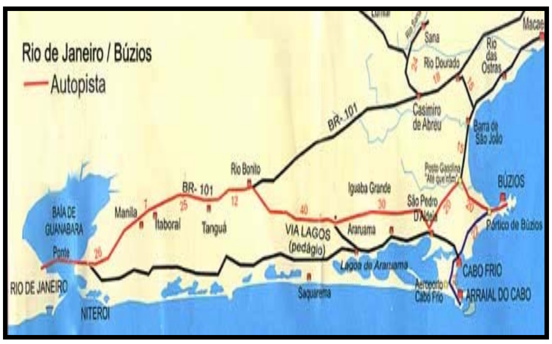

Fig.1 Map of the Rio-Niteroi bridge in the Guanabara bay.

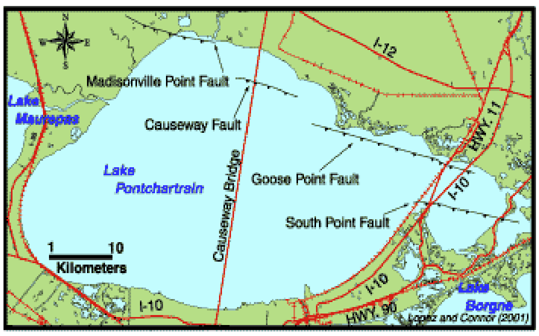

Fig.2 Map of the Causeway bridge over the Pontchartrain lake.

Fig.3 Aerial image of the Rio-Niteroi bridge in the Guanabara bay.

Fig.4 Aerial image of the Causeway bridge over the Pontchartrain lake.

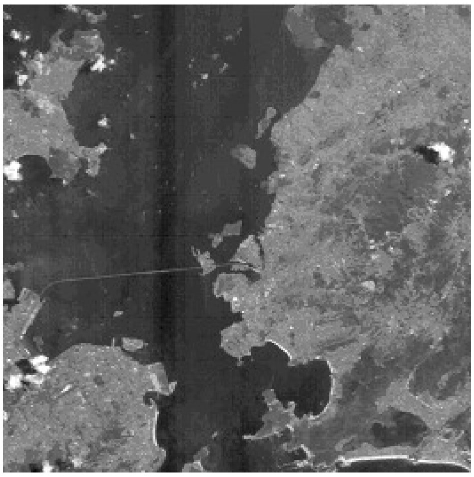

Fig.5 Band2 of Rio-Niteroi bridge destriped image captured by CBERS-1 CCD.

Fig.6 Band2 of Rio-Niteroi bridge original image captured by SPOT 4 CCD.

Fig.7 Band2 of Causeweay bridge destriped image captured by CBERS-1 CCD.

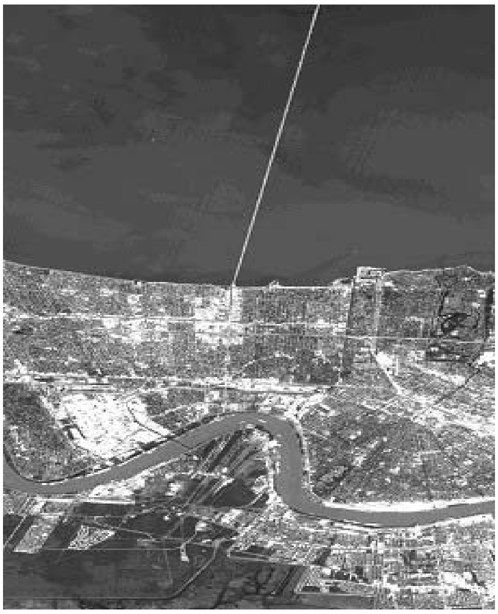

Fig.8 Band2 of Causeweay bridge original image captured by SPOT 4 CCD.

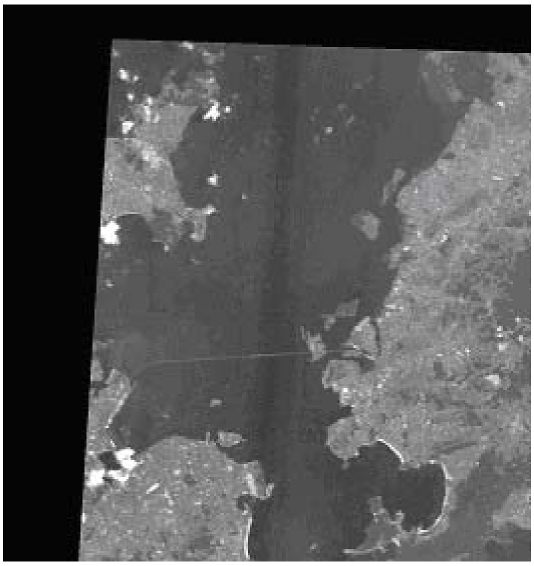

Fig.9 Registered band2
of the Rio-Niteroi bridge.

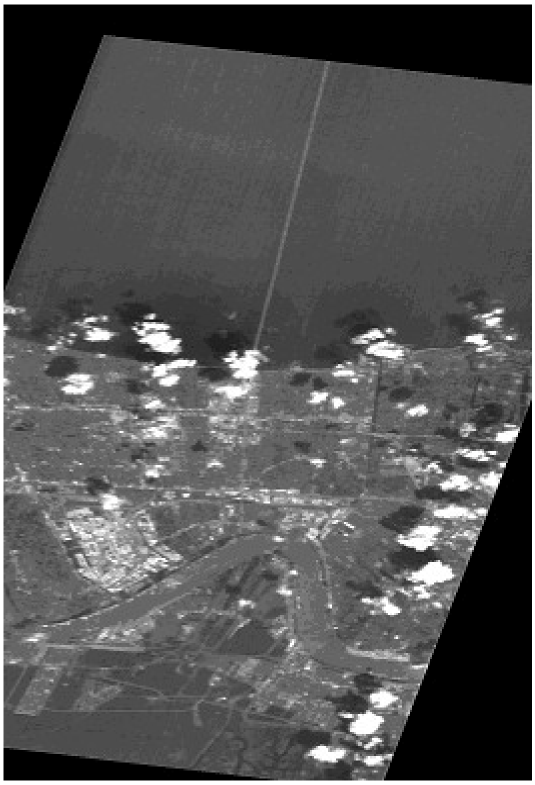

Fig.10 Registered band2
of the Causeway bridge.

3.4 Point spread function modelling

The overall on-orbit PSF is the convolution of each sub-system PSF: optic, detector, electronic, etc. In this work the point spread function is modeled as a 2D separable Gaussian function that is,

$$h(x_1, x_2) = h_{\sigma_1}(x_1).h_{\sigma_2}(x_2),$$

where

$$h_\sigma(x) = \frac{1}{\sqrt{2\pi}\,\sigma} e^{-\frac{x^2}{2\sigma^2}} \quad .$$

In this work, the employed method for the CBERS-1 EIFOV estimation is based on the degradation of a SPOT-4 image. It assumes that the CBERS-1 and SPOT-4 image are registered and that the SPOT EIFOV of each band is known.
Let f be the original scene and let h_s be the SPOT-4 imaging system PSF. Then the original SPOT-4 image is given by:

$$g_s = h_s * f \ .$$

Let h_d be the degradation filter PSF. Then the SPOT-4 degraded image is given by:

$$g_d = h_d * g_s = h_d * (h_s * h_f) = (h_d * h_s) * f \ .$$

Finally, let h_c the CBERS-1 imaging system PSF. Then, the CBERS-1 image is given by:

$$g_c = h_c * f \ .$$

To find the PSF of CBERS-1 imaging system h_c, we minimize the difference between the CBERS-1 image g_c and the SPOT-4 degraded image g_d by adjusting h_d. At the minimum, $g_d \approx g_c$ and $h_s * h_d$ is our estimation for h_c. The **figure 11** shows the block diagram of low-resolution image simulation.

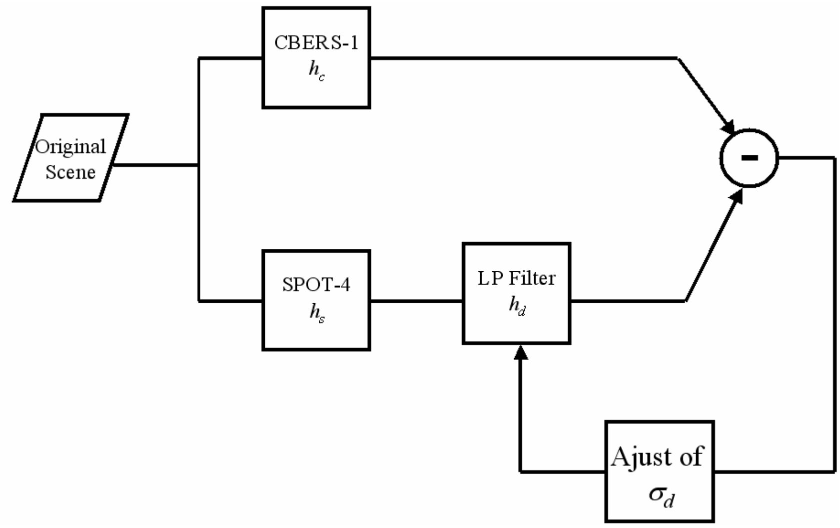

Fig.11 block diagram of low-resolution image simulation

For the along-track and across-track spatial resolution estimation, a three-step approach was used. The first step consists of estimating a gain parameter for the radiometric adjust between CBERS-1 image and SPOT-4 image. The second step consists of finding an offset parameter that describes the residual registration error between both images. In the last step, the standard deviation parameter of degradation filter is estimated. This one is used to compute the EIFOV CBERS-1. In all steps the root-mean-square minimization is used. Details of the proposed method are presented below.

Let g_c be one column (respectively one line) of the along-track (respectively across-track) bridge CBERS-1 image and g_s be one column (respectively one line) of the along-track (respectively across-track) bridge SPOT-4 image.

Let denote by $g_{\mu,\sigma}$ be the degraded SPOT-4 column (respectively one line) that is:

$$g_{\mu,\sigma} = h_{\mu,\sigma} * g_s ,$$

where $h_{\mu,\sigma}(x) = h_\sigma(x-\mu)$.

Step 1: Radiometric Adjust

In this step, the radiometric adjust is based on the estimation of a gain parameter a that allows to minimize the radiometry difference between the CBERS-1 column (respectively line) and the SPOT-4 column (respectively line).

Hence, given an a priori value σ_0 we look for the parameter a which minimizes

$$\sum \left(\left(a g_c + b \right) - g_{o,\sigma_0} \right)^2 ,$$

where $b = m - a.m_c$ (the initial value for a in the minimization is s/s_c), m_c and s_c are the mean and standard deviation of g_c, and m and s are the mean and standard deviation of g_s.

Step 2: Offset Adjust

In this step a and b being the parameters found at step 1, we look for μ that minimizes

$$\sum\left(\left(ag_c + b\right) - g_{\mu,\sigma_0}\right)^2$$

Step 3: EIFOV Estimation

In this step a, b and μ being the parameters found in the previous steps we look for σ that minimizes

$$\sum\left(\left(ag_c + b\right) - g_{\mu,\sigma}\right)^2$$

The along-track (respectively across-track) EIFOV estimation of CBERS-1 imaging system is given by:

$$\text{EIFOV}_c = 2.66\left(\left(\frac{\text{EIFOV}_s}{2.66}\right)^2 + \sigma^2\right)^{1/2}$$

where EIFOVs is the along-track (respectively across-track) spatial resolution of SPOT-4 imaging system.

The final estimated value of the imaging system EIFOV_c is the mean value of the EIFOVc obtained at each column (respectively each line).

In the three steps, the parameters have been obtained by nonlinear programming (Himmelblau, 1972).

4. Results

Table 2 and **Table 3** present the EIFOV values of SPOT-4 imaging system used in this work. The results of the estimated parameters of CBERS-1 CCD imaging system are presented in **Table 4** and **Table 5**.

Table 2: SPOT-4 EIFOVs in along-track direction.

Bands	σ_1	EIFOV_1
B2	10.56	28
B3	11.26	30
B4	11.63	31

Table 3: SPOT-4 EIFOVs in across-track direction.

Bands	σ_2	EIFOV_2
B2	10	27
B3	10.7	29
B4	12.6	34

Table 4: CBERS-1 estimated EIFOVs in along-track direction.

Bands	σ_1	EIFOV_1
B2	12.74	34
B3	13.8	37
B4	20.3	54

Table 5: CBERS-1 estimated EIFOVs in across-track direction.

Bands	σ_2	EIFOV_2
B2	24.34	65
B3	24.1	64
B4	28.75	77

5. Conclusion

An algorithm for the spatial resolution estimation of CBERS-1 CCD imaging system was presented. The proposed algorithm consisted of simulating a low resolution CBERS-1 image from a higher resolution SPOT-4 image. Our results confirm EIFOV's values obtained in the previous work (Bensebaa et al, 2004a, b). In along-track-direction the imaging system spatial resolution is in specifications for all bands except band 4. In across-track direction the imaging system spatial resolution is out of the specifications for all bands.

References

Banon, G. J. F. Simulação de imagens de baixa resolução. **Controle & Automação**, v. 2, n. 3, p. 180-192, March/April 1990.

Banon, G. J. F.; Santos, A. C. **Digital filter design for sensor simulation**: application to the Brazilian Remote Sensing Satellite. Sao Jose dos campos: INPE, 1993. 62 p. (INPE-5523-RPQ/665). Disponível na biblioteca digital UR*Lib*: <dpi.inpe.br/banon/1995/12.14.18.12>. Acesso em: 18 nov. 2004.

Bensebaa, K.; Banon, G. J. F.; Fonseca, L. M. G. On-orbit spatial resolution estimation of CBERS-1 CCD imaging system. Accepted for publication in the Third International Conference on Image and Graphics, Hong Kong, China, 2004.

Bensebaa, K.; Banon, G. J. F.; Fonseca, L. M. G. On-orbit Spatial Resolution Estimation of CBERS-1 CCD Imaging System from bridge images. In: International Society for Photogrammetry and Remote Sensing (ISPRS), 20., 12-23 July 2004, Istanbul, Turkey. **Proceedings…** 2004. v. 35, Part B1, p. 36-41.

Choi, T.; Helder, D. L. Techniques for measuring the in-orbit modulation transfer function (MTF) for high spatial resolution imaging satellite. In: High Spatial Resolution Commercial Imagery Workshop, Mar. 2001, Greenbelt, USA. **Proceedings...** 2001.

Dayao, L.; Schaochun, C.; Shiju, J. China's satellite remote sensing technology and its application in 20^{th} century. In: Asian Conference in Remote Sensing, 22., 5-9 November 2001, Singapore. **Proceedings…** 2001.

Fedorov, D.; Fonseca, L. M. G.; Kenney, C.; Manjunath, B. S. Automatic registration and mosaicking system for remotely sensed imagery. In: Simpósio Brasileiro de Sensoriamento Remoto, 11., 5-10 abr. 2003, Belo Horizonte. **Anais**... São José dos Campos: INPE, 2003. p. 1771-1779. CD-ROM. Publicado como: INPE-10534-PRE/6006. Disponível na biblioteca digital UR*Lib*: <ltid.inpe.br/sbsr/2002/11.18.09.27>. Acesso em: 18 nov. 2004.

Fonseca, L. M. G. **Determinação e avaliação das funções de transferência de modulação (MTF) dos sistemas MSS e TM (Landsat-5)**. São Jose dos Campos: INPE, 1987. 19 p. (INPE-4187-RPE/543).

Fonseca, L. M. G.; Mascarenhas, N. D. D. Determinação da função de transferência do sensor TM do satélite Landsat-5. In: Congresso Nacional de Matemática Aplicada e Computacional, 10., 21-26 set. 1987, Gramado, BR. **Resumo dos Trabalhos**... 1987. p. 297-302. Publicado como: INPE-4213-PRE/1094.

Himmelblau, D. M. **Applied Nonlinear Programming**. New York: McGraw-Hill Book Company, 1972.

Leger, D.; Viallefont-Robinet, F.; Meygret, A. In-flight refocusing and MTF assessment of SPOT5 HRG and HRS cameras, In: International Symposium on Remote sensing, 9., Sep. 2002, Aghia Pelagia, Greece. **Proceedings…** 2002.

Luxen, M.; Forstner,. **Characterizing image quality: blind estimation of the point spread function from a single image**. Institute for Photogrammetry, University of Bonn, Germany.

Storey, J. C. Landsat 7 on-orbit modulation transfer function estimation. In: Sensors, Systems, and Next Generation Satellites V, 17-20 Sep. 2001, Toulouse, France. **Proceedings..**. Bellingham, WA, USA: SPIE, 2001. p. 50-61.